

Variational Quantum Operator Simulation

Satoru Shoji,^{1,*} Kosuke Ito,² Yukihiro Shimizu,^{1,†} and Keisuke Fujii^{2,3,4}

¹*Department of Applied Physics, Graduate School of Engineering, Tohoku University, Sendai 980-8579, Japan*

²*Center for Quantum Information and Quantum Biology,
International Advanced Research Institute, 1-2 Machikaneyama,
Toyonaka, Osaka University, Osaka 560-8531, Japan*

³*Graduate School of Engineering Science, Osaka University,
1-3 Machikaneyama, Toyonaka, Osaka 560-8531, Japan*

⁴*RIKEN Center for Quantum Computing (RQC), Hirosawa 2-1, Wako, Saitama 351-0198, Japan*

(Dated: March 9, 2026)

Implementing time-evolution operators in shallow quantum circuits is important for quantum simulations. The standard method of Trotterization requires a large number of gates to achieve practical accuracy. Variational Quantum Simulation (VQS) is an algorithm that calculates the time evolution of a quantum state and can be executed with shallower circuits than Trotterization. However, the operator obtained by VQS evolves only a fixed initial state and is not the time evolution operator itself. In this paper, we propose Variational Quantum Operator Simulation (VQOS), a method to realize time evolution operators in shallow quantum circuits. This method is based on the variational principle for operators and does not require the implementation of the desired Trotter decomposition of the time evolution operator. We performed numerical simulations of the VQOS algorithm and successfully implemented the time evolution operator for closed systems in a quantum circuit that is up to 5 times shallower than the Trotterization. By providing a more practical way to implement time evolution operators, VQOS increases the applicability of near-term quantum computers.

I. INTRODUCTION

Quantum computers are expected to offer advantages over classical computers for certain computational tasks. In particular, Hamiltonian simulation and eigenvalue problems play a central role in quantum science, and quantum algorithms for these tasks have attracted significant attention [1, 2]. While classical algorithms and approximation methods are available for many physically relevant systems, quantum approaches may provide favorable scaling or practical advantages in regimes where classical simulations become challenging. Rather than claiming asymptotic quantum advantage, our focus is on reducing circuit depth and avoiding oracle access in near-term settings. In particular, the implementation of time-evolution operators as quantum circuits plays a crucial role not only in the simulations of quantum dynamics but also as a key component of quantum phase estimation [3] and quantum eigenvalue transformation of unitaries [4]. By using the Trotterization [5, 6], the time evolution operators can be approximated as a quantum circuit. This is one of the simplest approaches, but it requires a very large number of gates, and it is not realistic to implement long-time evolution operators with sufficient accuracy before full fault tolerance [7, 8].

Regarding algorithms for near-term quantum devices, one approach is Quantum Assisted Quantum Compiling (QAQC) [9]. This method compiles the time evolution operators approximately into a variational quantum cir-

cuit via the minimization of the cost function given by the distance from the true time evolution operator. However, this method requires oracle access to the target time evolution operator as a quantum circuit, which is a difficult problem in itself. Furthermore, the number of circuits to be evaluated to obtain a compiled circuit cannot be known in advance, and optimization may fail due to local minima or a barren plateau [10] (exponentially vanishing gradient) in the cost function. Local variational quantum compilation (LVQC) [11, 12], a variant of QAQC, uses a Lieb-Robinson bound and causal cones to reduce the effective number of qubits, and the parameters of the variational quantum circuit are optimized by a classical simulator, which requires a large classical computation. Therefore, for near-term applications, it is essential to develop an algorithm that approximates the time evolution operator using a shallow circuit, without requiring prior preparation of the target operator in either quantum circuits or classical computations.

Another approach for dynamics simulation is variational quantum simulation (VQS) [13–16]. The VQS simulates the time evolution of a quantum state using the variational principle. This method does not require prior preparation of the target operator in quantum circuits. However, VQS only yields the time evolution of a fixed initial state, not the time evolution operator itself. In other words, the quantum circuit obtained by VQS approximates the time evolution from a predetermined state but does not correctly time-evolve another initial state. Therefore, VQS cannot be used for quantum phase estimation or long-time evolution via repeated application of the time-evolution operator.

To address the above issues, this paper proposes Varia-

* Contact author: satoru.shoji.t8@dc.tohoku.ac.jp

† Contact author: shimizu@tohoku.ac.jp

tional Quantum Operator Simulation (VQOS), a method to variationally approximate the target time evolution operator itself without oracle access to the target time evolution operator. In this paper, we refer to the ordinary VQS as Variational Quantum State Simulation (VQSS), in contrast to VQOS. Similarly to VQSS, VQOS does not require oracle access to the target time evolution operator nor classical optimization of a cost function. Hence, it is free from trainability problems such as local solutions and the barren plateau. Furthermore, the number of quantum circuits required to run VQOS can be pre-computed from the Hamiltonian and number of variational parameters. This is achieved by applying the variational principle of the time evolution operator to a parameterized quantum circuit (ansatz) $U(\boldsymbol{\theta}(t))$. Although the formulation is formally equivalent to applying VQSS to the Choi state, the actual implementation can be performed on a single system without entangled inputs, resulting in a simpler and shallower circuit.

We assess the performance of VQOS through classical simulations of the transverse-field Heisenberg model with up to nine sites. The results demonstrate that VQOS achieves up to three orders of magnitude improvement in accuracy compared to Trotterization, given the same circuit depth. Additionally, VQOS is capable of approximating the time-evolution operator with comparable accuracy to that of Trotterization while requiring only approximately one-quarter of the circuit depth. Importantly, the degradation in accuracy due to increasing system size was found to be minimal, indicating favorable scalability of the method.

The remainder of this paper is organized as follows. Sec. II briefly summarizes the VQSS. Sec. III introduces the VQOS method, and Sec. IV proposes circuit implementations for VQOS, Sec. V presents the numerical results of applying VQOS to the transverse field Heisenberg model. Finally, Sec. VI summarizes the paper.

II. BRIEF REVIEW OF THE VQSS

VQS [13, 14] is a quantum–classical hybrid algorithm used to approximate the time evolution of a quantum system from a fixed initial state based on the variational principle. We refer to this conventional VQS as VQSS.

A. Formulations

The target problem is to solve the time-dependent Schrödinger equation

$$\frac{d}{dt} |\psi(t)\rangle = -iH |\psi(t)\rangle, \quad (1)$$

with Hamiltonian H and an initial state $|\phi_{\text{in}}\rangle = |\psi(0)\rangle$. In VQSS, an ansatz

$$|\phi(\theta_0(t), \boldsymbol{\theta}(t))\rangle = e^{i\theta_0(t)} U(\boldsymbol{\theta}(t)) |\phi_{\text{in}}\rangle, \quad (2)$$

approximates the exact time evolution $|\psi(t)\rangle$. Here, $U(\boldsymbol{\theta}(t))$ is a parameterized unitary gate. The parameters are represented as a real vector of length N_{params} . In Eq. (2), the global phase $e^{i\theta_0(t)}$ is introduced to deal with the global phase mismatch pointed out in Ref. [14]. Although VQSS can also be applied to time-dependent Hamiltonians, we focus on the time-independent case here for simplicity. We use McLachlan’s variational principle [17]

$$\delta \left\| \frac{d}{dt} |\phi(\theta_0(t), \boldsymbol{\theta}(t))\rangle + iH |\phi(\theta_0(t), \boldsymbol{\theta}(t))\rangle \right\| = 0, \quad (3)$$

to find parameters $\boldsymbol{\theta}(t)$ that approximately satisfy Eq. (1) within the expressibility of the ansatz. Although there are other variational principles, we use McLachlan’s due to its consistency with open systems [14]. As a result, we obtain a formula for updating the variational parameters

$$M\dot{\boldsymbol{\theta}} = V. \quad (4)$$

Here, each element of the real symmetric matrix M and real vector V can be written as follows:

$$M_{j,k} = \text{Re} \left(\frac{\partial \langle \phi(\boldsymbol{\theta}) |}{\partial \theta_j} \frac{\partial |\phi(\boldsymbol{\theta})\rangle}{\partial \theta_k} \right) + \frac{\partial \langle \phi(\boldsymbol{\theta}) |}{\partial \theta_j} |\phi(\boldsymbol{\theta})\rangle \frac{\partial \langle \phi(\boldsymbol{\theta}) |}{\partial \theta_k} |\phi(\boldsymbol{\theta})\rangle, \quad (5)$$

$$V_k = \text{Im} \left(\frac{\partial \langle \phi(\boldsymbol{\theta}) |}{\partial \theta_k} H |\phi(\boldsymbol{\theta})\rangle \right) + i \frac{\partial \langle \phi(\boldsymbol{\theta}) |}{\partial \theta_k} |\phi(\boldsymbol{\theta})\rangle \langle \phi(\boldsymbol{\theta}) | H |\phi(\boldsymbol{\theta})\rangle. \quad (6)$$

Here, M is an $N_{\text{params}} \times N_{\text{params}}$ matrix, and V is a length N_{params} vector. Note that because $\frac{\partial \langle \phi(\boldsymbol{\theta}) |}{\partial \theta_j} |\phi(\boldsymbol{\theta})\rangle$ in Eqs. (5) and (6) is pure imaginary, M and V are a real matrix and vector, respectively. In the VQSS, we estimate M and V using quantum computers. Then, Eq. (4) is solved classically. The implementation of the quantum circuit to estimate M and V is described in detail in a later section.

Using an ansatz with sufficiently high expressibility, we get variational parameters $\boldsymbol{\theta}(t)$ that approximate the time evolution of states. For example, for VQSS of closed systems, the approximation

$$e^{-iHt} |\phi_{\text{in}}\rangle \approx U(\boldsymbol{\theta}(t)) |\phi_{\text{in}}\rangle \quad (7)$$

is satisfied. However, the operator $U(\boldsymbol{\theta}(t))$ obtained by VQSS with the initial state $|\phi_{\text{in}}\rangle$ does not necessarily give the correct time evolution for another different initial state. In other words, because VQSS does not approximate the time evolution operator itself, $e^{-iHt} \approx U(\boldsymbol{\theta}(t))$ is generally not satisfied. Therefore, to compute the time evolution from different initial states, we must execute VQSS for each of them. Also, the $U(\boldsymbol{\theta}(t))$ obtained by VQSS cannot be used for algorithms such as quantum phase estimation.

B. Implementations

In VQSS, we estimate Eqs. (5) and (6) using quantum computation. Suppose that the ansatz

$$|\phi(\boldsymbol{\theta})\rangle = R_L(\theta_L) \cdots R_1(\theta_1) |\phi_{\text{in}}\rangle, \quad (8)$$

is represented by the product of the rotation gates $R_j(\theta_j) = \exp(iG_j\theta_j)$, defined by L Pauli operators $G_j \in \{I, X, Y, Z\}^{\otimes n}$. We also suppose that the Hamiltonian

$$H = \sum_j c_j H_j, \quad (9)$$

is written as a linear combination of Pauli operators $H_j \in \{I, X, Y, Z\}^{\otimes n}$ with real coefficients c_j . Then, Eqs. (5) and (6) can be written as

$$\begin{aligned} M_{jk} &= \text{Re} \langle \phi_{\text{in}} | U_{j-1:1}^\dagger G_j U_{k-1:j}^\dagger G_k U_{k-1:1} | \phi_{\text{in}} \rangle \\ &\quad - \langle \phi_{\text{in}} | U_{j-1:1}^\dagger G_j U_{j-1:1} | \phi_{\text{in}} \rangle \\ &\quad \times \langle \phi_{\text{in}} | U_{k-1:1}^\dagger G_j U_{k-1:1} | \phi_{\text{in}} \rangle, \end{aligned} \quad (10)$$

$$\begin{aligned} V_j &= - \sum_k c_k \text{Re} \langle \phi_{\text{in}} | U_{j-1:1}^\dagger G_j U_{L:j}^\dagger H_k U_{L:1} | \phi_{\text{in}} \rangle \\ &\quad + \langle \phi_{\text{in}} | U_{j-1:1}^\dagger G_j U_{j-1:1} | \phi_{\text{in}} \rangle \\ &\quad \times \sum_k c_k \langle \phi_{\text{in}} | H_k | \phi_{\text{in}} \rangle, \end{aligned} \quad (11)$$

where $R_k(\theta_k) \cdots R_j(\theta_j)$ is written as $U_{k:j}$. The first terms of Eqs. (10) and (11) can be expressed as a linear combination of

$$g_{jkl} = \text{Re} \langle \phi_{\text{in}} | U_{j-1:1}^\dagger P_j U_{l:j}^\dagger P_k U_{l:1} | \phi_{\text{in}} \rangle. \quad (12)$$

This quantity can be estimated either by an indirect measurement method via a Hadamard test with two controlled gates [14] (Fig. 1(a)) or by a direct measurement method [18] (Fig. 1(b)). The second terms of Eqs. (10) and (11) can be evaluated by estimating the expectation values $\langle \phi_{\text{in}} | U_{j-1:1}^\dagger G_j U_{j-1:1} | \phi_{\text{in}} \rangle$, and $\langle \phi_{\text{in}} | H_k | \phi_{\text{in}} \rangle$.

III. VARIATIONAL QUANTUM OPERATOR SIMULATION

In this section, we show that the time evolution operator can be approximated by VQOS. The objective of VQOS is to find a parameter $\boldsymbol{\theta}(t)$ of the circuit $\tilde{U}(\boldsymbol{\theta}(t)) = e^{i\theta_0(t)} U(\boldsymbol{\theta}(t))$ that approximates

$$e^{-iHt} |\phi_{\text{in}}\rangle \approx \tilde{U}(\boldsymbol{\theta}(t)) |\phi_{\text{in}}\rangle, \quad (13)$$

for any initial state $|\phi_{\text{in}}\rangle$. Here we consider a d -dimensional system. In Eq. (13), the global phase factor $e^{i\theta_0(t)}$ is introduced, as in the case of VQSS, to address

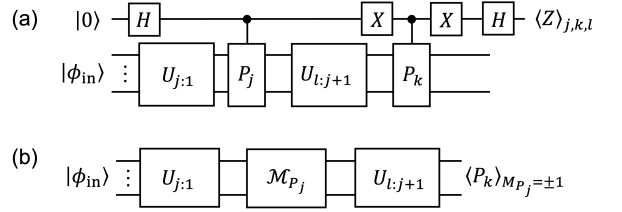


FIG. 1. Circuits to estimate Eq. (12). (a) Indirect measurement method. g_{jkl} is estimated by measuring ancilla qubit $\langle Z \rangle_{j,k,l}$. (b) Direct measurement method. \mathcal{M}_{P_j} is the measurement with Pauli operator P_j . g_{jkl} is estimated as $p(M_{P_j} = +1)\langle P_k \rangle_{M_{P_j}=+1} - p(M_{P_j} = -1)\langle P_k \rangle_{M_{P_j}=-1}$. $p(M_{P_j} = \pm 1)$ is the probability that the outcome of the mid-measurement is ± 1 . $\langle P_k \rangle_{M_{P_j}=\pm 1}$ is the expectation value of P_k conditional on $M_{P_j} = \pm 1$.

the mismatch in the global phase. Eq. (13) can be expressed as follows:

$$\delta \left\| \frac{d}{dt} \tilde{U}(\boldsymbol{\theta}(t)) + iH\tilde{U}(\boldsymbol{\theta}(t)) \right\|_{\text{F}} = 0. \quad (14)$$

Eq. (14) gives the equation of VQOS, which describes the time evolution of parameters,

$$N\dot{\boldsymbol{\theta}} = W, \quad (15)$$

where

$$\begin{aligned} N_{jk} &= \text{Re} \text{Tr} \left[\left(\frac{\partial U(\boldsymbol{\theta})}{\partial \theta_j} \right)^\dagger \frac{\partial U(\boldsymbol{\theta})}{\partial \theta_k} \right] \\ &\quad + \frac{1}{2^n} \text{Tr} \left[\left(\frac{\partial U(\boldsymbol{\theta})}{\partial \theta_j} \right)^\dagger U(\boldsymbol{\theta}) \right] \\ &\quad \times \text{Tr} \left[\left(\frac{\partial U(\boldsymbol{\theta})}{\partial \theta_k} \right)^\dagger U(\boldsymbol{\theta}) \right], \end{aligned} \quad (16)$$

$$\begin{aligned} W_j &= \text{Im} \text{Tr} \left[\left(\frac{\partial U(\boldsymbol{\theta})}{\partial \theta_j} \right)^\dagger H U(\boldsymbol{\theta}) \right] \\ &\quad - \frac{\cos(\theta_0)}{2^n} \text{Tr} \left[\left(\frac{\partial U(\boldsymbol{\theta})}{\partial \theta_j} \right)^\dagger U(\boldsymbol{\theta}) \right] \text{Tr}[H]. \end{aligned} \quad (17)$$

Here, because $\left(\frac{\partial U(\boldsymbol{\theta})}{\partial \theta_j} \right)^\dagger U(\boldsymbol{\theta})$ is anti-Hermitian, N and W are a real matrix and vector, respectively. The trace of the Hamiltonian contributes only to a global phase. Thus, without loss of generality, we may assume $\text{Tr}[H] = 0$, such that the second term of Eq. (17) vanishes.

The evolution by Eq. (15) is equivalent to applying VQSS of the Choi state [19, 20]. More specifically, the time evolution of VQSS with Hamiltonian $H \otimes I$ (I is the identity operator with the same size as H) and initial state as the maximally entangled state

$$|\Phi\rangle = \frac{1}{\sqrt{d}} \sum_{j=0}^{d-1} |j\rangle \otimes |j\rangle, \quad (18)$$

is equivalent to VQOS. This equivalence can be confirmed by setting ansatz $|\phi(\boldsymbol{\theta}(t))\rangle$ to $(\tilde{U}(\boldsymbol{\theta}(t)) \otimes I)|\Phi\rangle$ and the Hamiltonian H to $H \otimes I$ in Eq. (3):

$$\delta \left\| \frac{d}{dt} (\tilde{U}(\boldsymbol{\theta}(t)) \otimes I) |\Phi\rangle + i(H \otimes I)(\tilde{U}(\boldsymbol{\theta}(t)) \otimes I) |\Phi\rangle \right\| = \frac{1}{\sqrt{d}} \delta \left\| \frac{d}{dt} \tilde{U}(\boldsymbol{\theta}(t)) + iH\tilde{U}(\boldsymbol{\theta}(t)) \right\|_{\mathbb{F}} = 0, \quad (19)$$

which leads to the same variational principle used in VQOS for pure states, as shown in Eq. (14). Here, in Eq. (19), d is the dimension of the system we are now interested in, and we use the relation $\langle \Phi | (A \otimes I) | \Phi \rangle = \text{Tr}(A)/d$ that holds for a general square matrix A . This equivalence might suggest that VQOS must be implemented by performing VQSS on the Choi state, which would require preparing a maximally entangled input state. However, as explained in Sec. IV, this is not necessary. VQOS can be implemented on a single d -dimensional system (i.e., an n -qubit register) without entangled inputs.

IV. IMPLEMENTATION

In this section, we describe the implementation of VQOS to approximate the time evolution operators e^{-iHt} under an n -qubit Hamiltonian H . In order to implement VQOS, we need to compute N_{jk} and W_j defined in Eqs. (16) and (17), respectively. Similarly to Eqs. (8) and (9), we suppose that the variational quantum circuit $U(\boldsymbol{\theta})$ is represented by the product of the rotation gates as $U(\boldsymbol{\theta}) = R_L(\theta_L) \cdots R_1(\theta_1)$ where $R_j(\theta_j) = \exp(iG_j\theta_j)$ is defined by L Pauli operators $G_j \in \{I, X, Y, Z\}^{\otimes n}$ and the Hamiltonian H can be expressed by a linear combination of n_H Pauli operators $H_k \in \{I, X, Y, Z\}^{\otimes n}$ with real coefficients c_j . Under the above assumptions, these quantities are written as

$$N_{jk} = \frac{1}{2^n} \text{Re} \left[\text{Tr} \left(G_j U_{k:j+1}^\dagger G_k U_{k:j+1} \right) \right], \quad (20)$$

$$W_j = \frac{1}{2^n} \sum_{k=1}^{n_H} c_j \text{Re} \left[\text{Tr} \left(P_j U_{L:j+1}^\dagger H_k U_{L:j+1} \right) \right], \quad (21)$$

where we define $U_{k:j} := R_k(\theta_k) \cdots R_j(\theta_j)$. Because both N and W can be written by a linear combination of

$$g_{jkl} := \frac{1}{2^n} \text{Re} \left[\text{Tr} \left(P_j U_{l:j+1}^\dagger P_k U_{l:j+1} \right) \right], \quad (22)$$

where $P_j, P_k \in \{I, X, Y, Z\}^{\otimes n}$, N and W can be obtained by estimating g_{jkl} .

Although g_{jkl} can be estimated by implementing VQSS of the Choi state using n Bell pairs as suggested by the equivalence shown in Sec. III, VQOS admits more efficient implementations on a single n -qubit register without any entangled input state, as already implied by Eq. (22). As shown below, VQOS can be implemented

by the reduced circuits in Fig. 2(a) and Fig. 2(b), requiring $n+1$ qubits for the indirect measurement method and n qubits for the direct measurement method. Compared with directly implementing VQSS on the Choi state (Fig. 2(a') and Fig. 2(b')), these reduced circuits eliminate the entangled input and the idling register, and they are also shallower.

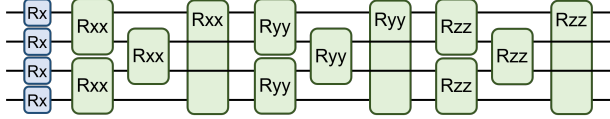
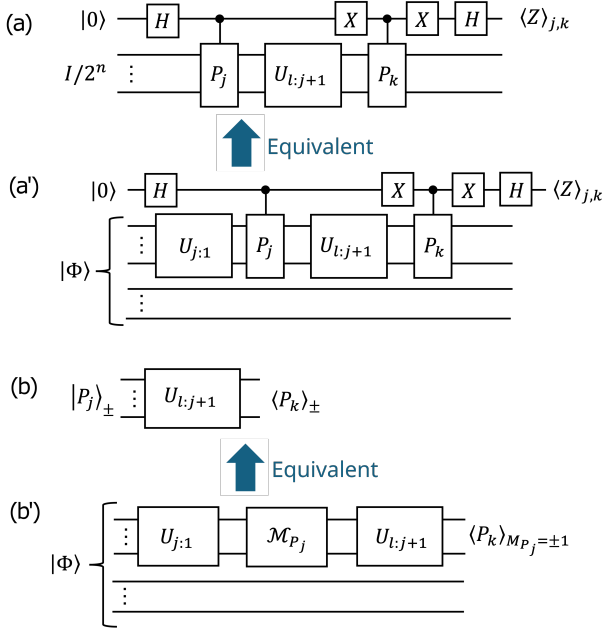
First, we consider the indirect measurement method [13, 14] using a single ancilla qubit. In the circuit implementation obtained by directly applying the indirect measurement method of VQSS to the Choi state (Fig. 2(a')), gate operations and measurements are not performed on one qubit of each Bell pair. Hence, we can trace out those idling qubits to obtain the equivalent reduced circuit shown in Fig. 2(a). This shows that the indirect measurement implementation only requires an n -qubit maximally mixed input state. Moreover, the circuit depth is reduced because the first j layers $U_{j:1}$ can be omitted since it acts only on the maximally mixed state and therefore does not affect g_{jkl} .

Second, the direct measurement method [18] also admits a simpler circuit implementation. Again, if one directly applies the direct measurement method of VQSS to the Choi state (Fig. 2(b')), no manipulation is performed on one qubit of each Bell pair, and tracing out those qubits yields an equivalent reduced circuit. Furthermore, in Fig. 2(b') the expectation value of P_j is measured in the middle of the circuit. In VQOS, this intermediate measurement can be removed by replacing it with random initialization in eigenstates of P_j . More precisely, the input state is chosen uniformly at random as $|P_j\rangle_+$ or $|P_j\rangle_-$ with eigenvalue $+1$ or -1 of P_j . Let $\langle P_k \rangle_+$ and $\langle P_k \rangle_-$ be the expectation values of the final measurement of P_k when the initial state is $|P_j\rangle_+$ and $|P_j\rangle_-$, respectively. Then g_{jkl} can be estimated as $(\langle P_k \rangle_+ - \langle P_k \rangle_-)/2$, leading to the reduced circuit in Fig. 2(b). This implementation requires only an n -qubit register with shallower circuit $U_{l:j+1}$ and eliminates both the entangled input state and the intermediate measurement.

We also remark that the number of circuits to be evaluated in VQOS is less than that with VQSS for the same number of parameters because the second terms in Eqs. (5) and (6) are trivially zero for VQOS using the ansatz in the form of Eq. (8). The number of quantum circuits required to run VQOS can be calculated in advance from the Hamiltonian and number of variational parameters. The number of quantum circuits required to estimate Eq. (20) is $L(L+1)/2$, and for Eq. (21), it is Ln_H .

V. NUMERICAL SIMULATION

In this section, we describe numerical calculations using VQOS to obtain time evolution operators. We adopt the 1D periodic boundary transverse magnetic field Heisenberg model as the system of interest. The Hamil-



tonian H is written as follows:

$$\begin{aligned}
 H &= -\frac{1}{2} \sum_{j=1}^n X_j - \frac{1}{2} \sum_{j=1}^n (X_j X_{j+1} + Y_j Y_{j+1} + Z_j Z_{j+1}) \\
 &= H_x + H_{xx} + H_{yy} + H_{zz}.
 \end{aligned} \tag{23}$$

Here, n is the number of sites, and the $(n+1)$ th site is considered the first site. The ansatz $U(\theta)$ (Fig. 3) has a one-to-one correspondence of sites to qubits and a circuit with the same configuration as the first-order

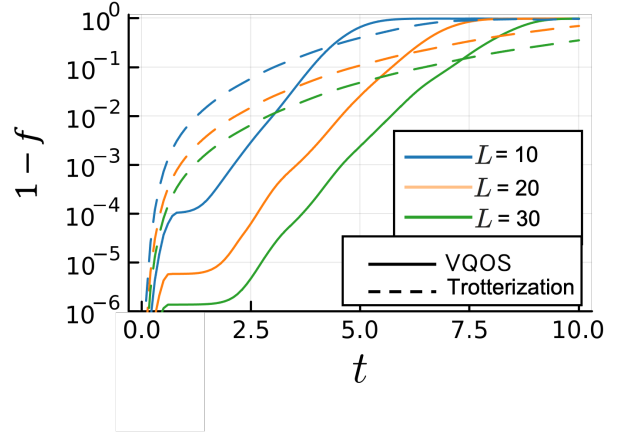


FIG. 4. The process infidelity $1 - f$ of the time evolution operators of the 9-site 1D periodic boundary transverse magnetic field Heisenberg model obtained by VQOS and Trotterization against the exact operator obtained by diagonalization of the Hamiltonian; the solid line is the result of VQOS, and the dotted line is the result of Trotterization. The blue, orange, and green plots correspond to 10, 20, and 30 layers, respectively.

Trotterization $U_{\text{trot}}(t, L)$, where

$$U_{\text{trot}}(t, L) = \left(e^{-iH_x t/L} e^{-iH_{xx} t/L} e^{-iH_{yy} t/L} e^{-iH_{zz} t/L} \right)^L \tag{24}$$

was used to compare the depths of the circuits. In Eq. (24), t and L denote time and number of layers, respectively. The parameters θ of the rotation gates in the ansatz $U(\theta)$ are different for each gate. In this study, we performed noiseless simulations using classical computers with the Yao.jl package [21]. Details about the numerical simulation are described in Appendix A.

Fig. 4 shows the error of the time evolution operator obtained by VQOS and Trotterization compared to the exact time evolution operator obtained by diagonalization of the Hamiltonian. The error of the two n -qubit operators U and V was evaluated by the process infidelity [22], which is defined as $1 - f = 1 - |\text{Tr}(V^\dagger U)|/2^n$. We found that in the range where the process infidelity is less than 10^{-1} , the VQOS error is always less than that of the Trotterization. We also found that the VQOS error increases exponentially with respect to t . This is thought to be because the increase in error due to sequential simulations is proportional to the current error. It can also be assumed that the ansatz has sufficient expressibility at the plateau that appears at the beginning of the simulation. Meanwhile, the error of Trotterization increases in proportion to the cube of t . This is because the leading term of the first-order Trotterization error is $\mathcal{O}(t^3)$. VQOS accuracy is worse than that of Trotterization in regions where operator infidelity is close to 1. This indicates that the variational principle simulation does not work well and does not find the optimal parameters within the range allowed by the trial function.

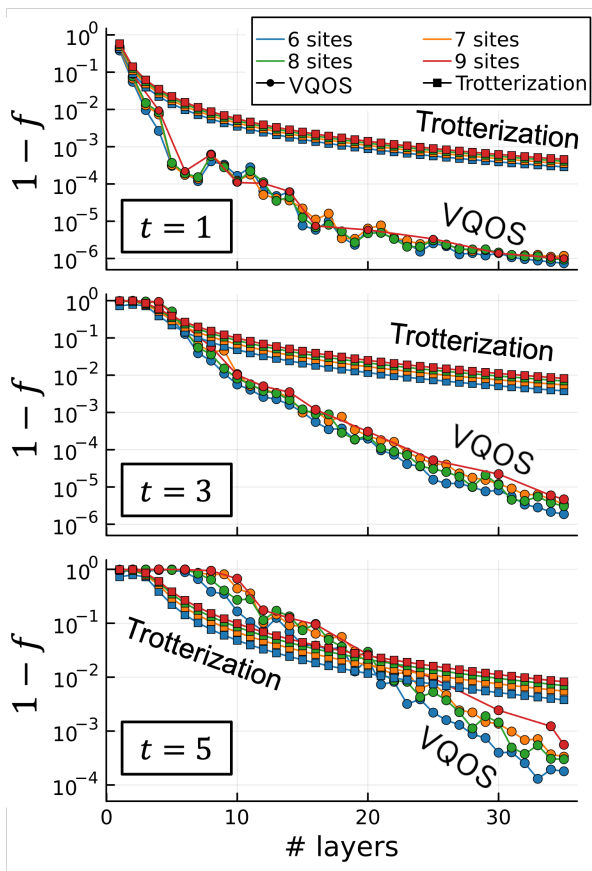


FIG. 5. Relationship between number of layers and operator infidelity $1-f$ at $t = 1, 3,$ and 5 in VQOS and Trotterization. Results for different sites correspond to different colored plots. The plots with round and square markers correspond to the results of VQOS and Trotterization, respectively.

Next, Fig. 5 shows the relationship between the number of layers and accuracy of VQOS and Trotterization. VQOS shows better accuracy than Trotterization except when t is large and the number of layers is small. When the number of layers is 30, the accuracy improves by a factor of 10 to 100. Furthermore, VQOS shows an exponential improvement in accuracy with increasing number of layers within the tested parameter range. In addition, when the number of sites is greater than 6, the difference in results among the number of sites is small. The difference in results between different numbers of sites increases as t increases, but the difference is not large at $t = 5$. Therefore, the number of layers required for VQOS is expected to scale slowly with increasing number of sites.

Finally, we discuss the number of layers required for VQOS. Fig. 6 shows the number of layers required to achieve process infidelity smaller than 10^{-3} in VQOS and Trotterization. The number of layers required in VQOS increases linearly with t at first and then saturates. The number of saturating layers increases rapidly with the

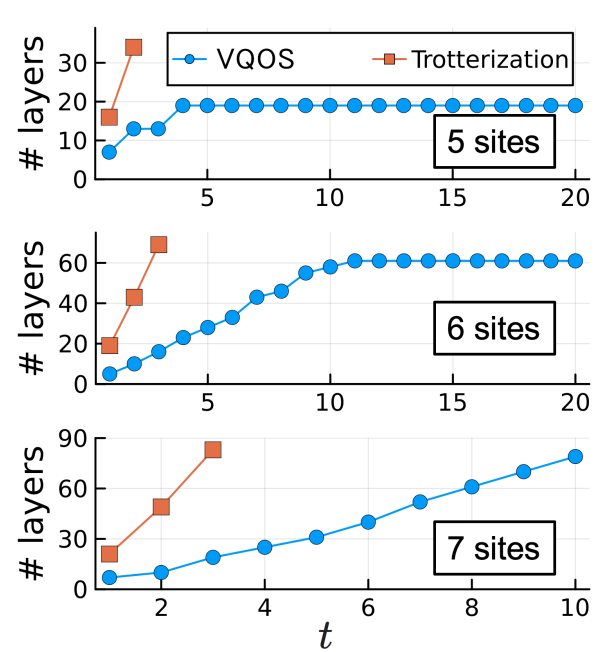


FIG. 6. Number of layers required to make operator infidelity $1-f$ smaller than 10^{-3} in VQOS and Trotterization for transverse field Heisenberg model with 5–7 sites. The plots with round and square markers correspond to the results of VQOS and Trotterization, respectively.

number of sites, and we could not find saturation in our calculations for more than 7 sites. In the saturating number of layers, the variational quantum circuit appears to have the ability to represent the time evolution operator in general time t . As the number of sites increases, the complexity of the general time evolution operator increases, and the number of saturating layers also increases. In any case, the number of layers required for VQOS is much less than for Trotterization.

VI. CONCLUSIONS

In this study, we developed VQOS, a method to approximate and implement the time evolution operator of a quantum system. We emphasize that VQOS is particularly suited for near-term applications in which (i) short- to intermediate-time evolution operators are required and (ii) explicit access to the time-evolution operator itself is essential, such as in quantum phase estimation and quantum eigenvalue transformation. The method was derived by applying McLachlan’s variational principle to a parameterized operator. It does not require another method to implement time evolution operators, such as Trotterization. Furthermore, it is not based on an iterative optimization of the cost functions but can be performed with a predetermined number of quantum operations. In addition, the circuit implementation of VQOS is resource-efficient. The algorithm can be ex-

cuted without Bell pairs or additional registers, resulting in shallower circuits than a naive Choi-state implementation.

Numerical results using VQOS to approximate the time evolution operator showed an accuracy improvement of up to 3 orders of magnitude or more for the same circuit depth compared to Trotterization, reducing the circuit depth by approximately 1/5 for the same accuracy comparison. In addition, it is suggested that the ansatz depth of VQOS can scale well with respect to the size of the system.

The method described in the main text of this paper can be extended to the dynamics of open quantum systems governed by the Lindblad equation. The corresponding formulation and implementation are presented in Appendix B.

Appendix A: Details of numerical simulations

In this study, we simulated VQOS on a classical computer. We used a method optimized for classical simulators that differs from the method mentioned in Sec. IV. That method reduces redundant computations by first obtaining the derivative of the ansatz $\frac{\partial|\phi(\boldsymbol{\theta})\rangle}{\partial\theta_j}$ for each parameter $\theta_j \in \boldsymbol{\theta}$, and then $\frac{\partial\langle\phi(\boldsymbol{\theta})|}{\partial\theta_j} H |\phi(\boldsymbol{\theta})\rangle$ and $\frac{\partial\langle\phi(\boldsymbol{\theta})|}{\partial\theta_j} H |\phi(\boldsymbol{\theta})\rangle$ are calculated. In this case, the computational cost to obtain N and W in Eq. (15) is linear with respect to the number of parameters L , while that of the method presented in the main text is $\mathcal{O}(L^2)$. This method requires the entire state vector to be stored and thus cannot be used in a real quantum computer.

Following [16], we added small values 10^{-8} to the diagonal components of N before solving Eq. (15) to avoid the numerical instability that comes with ill-conditioned N . The time step of integrating $\dot{\boldsymbol{\theta}}$ to obtain the time evolution of $\boldsymbol{\theta}$ was fixed at 0.05, and a fourth-order Runge-Kutta method was used.

Appendix B: Extension to open dynamics

VQOS can be extended to open quantum systems to find a channel $\mathcal{E}(\boldsymbol{\theta}(t))$ that approximates the time evolution of open systems based on the Lindblad equation, where $\mathcal{E}(\boldsymbol{\theta}(t))$ is the quantum channel parameterized by time-dependent parameters $\boldsymbol{\theta}(t)$. We call this method Variational Quantum Channel Simulation (VQCS). For this purpose, we use the following variational principle:

$$\delta \left\| \frac{d}{dt} \mathcal{E}(\boldsymbol{\theta}(t)) - \mathcal{L} \circ \mathcal{E}(\boldsymbol{\theta}(t)) \right\| = 0. \quad (\text{B1})$$

Here, we define the norm of a super-operator by

$$\|\mathcal{E}\| := \sum_a \text{Tr} [(\mathcal{E}(X_a))^\dagger \mathcal{E}(X_a)], \quad (\text{B2})$$

using the inner product of super-operators as defined in [23], where $\{X_a\}$ is an orthonormal basis of input systems

of \mathcal{E} . Using Eq. (B2), the variational principle of Eq. (B1) gives the equation of parameters for open systems

$$N\dot{\boldsymbol{\theta}} = W, \quad (\text{B3})$$

where

$$N_{jk} = \text{Tr} \left[\left(\frac{\partial \mathcal{E}(\boldsymbol{\theta})}{\partial \theta_j} \otimes \mathcal{I} \right) (|\Phi\rangle\langle\Phi|) \left(\frac{\partial \mathcal{E}(\boldsymbol{\theta})}{\partial \theta_k} \otimes \mathcal{I} \right) (|\Phi\rangle\langle\Phi|) \right], \quad (\text{B4})$$

$$W_j = \text{Tr} \left[\left(\frac{\partial \mathcal{E}(\boldsymbol{\theta})}{\partial \theta_j} \otimes \mathcal{I} \right) (|\Phi\rangle\langle\Phi|) \mathcal{L} \circ \mathcal{E}(\boldsymbol{\theta}) (|\Phi\rangle\langle\Phi|) \right] \quad (\text{B5})$$

\mathcal{I} is the identity channel. As in the closed system case, VQCS for open systems is also equivalent to the time evolution of the Choi state of $\mathcal{E}(\boldsymbol{\theta}(t))$ by Lindbladian $\mathcal{L} \circ \mathcal{I}$ in VQSS for open systems.

Next, we consider the implementation of VQCS for open systems. Because VQCS is equivalent to performing VQSS on the Choi states, we can use the implementation of VQSS proposed in [14]. Suppose that the parameterized quantum channel is given by $\mathcal{E}(\boldsymbol{\theta}) = \mathcal{R}_N(\theta_L) \cdots \mathcal{R}_1(\theta_1)$, where $\mathcal{R}_j(\theta_j)$ are quantum channels parameterized by a real parameter θ_j . We can rewrite the generator as

$$\mathcal{L}(\rho) = \sum_i g_i S_i \rho T_i^\dagger, \quad (\text{B6})$$

where S_i and T_i are unitary operators, and g_i are coefficients. Similarly, we write

$$\frac{\partial \mathcal{R}_k(\rho)}{\partial \theta_k} = \sum_i r_{k,i} S_{k,i} \rho T_{k,i}^\dagger, \quad (\text{B7})$$

where $S_{k,i}$ and $T_{k,i}$ are unitary operators, and $r_{k,i}$ are coefficients. N and W in Eq. (B3) can be expressed as

$$\begin{aligned} N_{k,q} &= \text{Re} (r_{k,i} r_{q,j} \text{Tr} [((\mathcal{R}_{k,i} \otimes \mathcal{I}) |\Phi\rangle\langle\Phi|) ((\mathcal{R}_{q,j} \otimes \mathcal{I}) |\Phi\rangle\langle\Phi|)]), \\ W_k &= \text{Re} (r_{k,i} g_j \text{Tr} [((\mathcal{R}_{k,i} \otimes \mathcal{I}) |\Phi\rangle\langle\Phi|) ((S_j \otimes \mathcal{I}) |\Phi\rangle\langle\Phi| (T_j^\dagger \otimes \mathcal{I}))]). \end{aligned} \quad (\text{B8})$$

Eq. (B8) can be evaluated by estimating

$$\text{Re} [e^{i\theta} \text{Tr}(\rho_1 \rho_2)], \quad (\text{B9})$$

where

$$\begin{aligned} \rho_1 &= (\mathcal{R}_N \cdots \mathcal{R}_{k+1} \otimes \mathcal{I}) [(S_k \otimes \mathcal{I}) ((\mathcal{R}_{k-1} \cdots \mathcal{R}_1 \otimes \mathcal{I}) |\Phi\rangle\langle\Phi|) (T_k^\dagger \otimes \mathcal{I})], \\ \rho_2 &= (\mathcal{R}_N \cdots \mathcal{R}_{q+1} \otimes \mathcal{I}) [(S_q \otimes \mathcal{I}) ((\mathcal{R}_{q-1} \cdots \mathcal{R}_1 \otimes \mathcal{I}) |\Phi\rangle\langle\Phi|) (T_q^\dagger \otimes \mathcal{I})]. \end{aligned} \quad (\text{B10})$$

As in the closed system case, because no gate operations are performed on half of the qubits, tracing them out results in the circuit shown in Fig. 7.

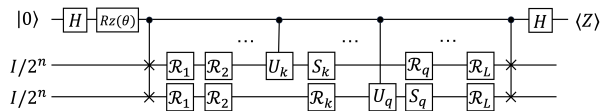


FIG. 7. Circuit for the evaluation of (B9) based on the circuit proposed in [14]. The ancillary qubit is initialized in the state $|0\rangle$, and both of the n qubit registers are initialized in the maximally mixed state $I/2^n$. Eq. (B9) is evaluated by estimating the expectation value $\langle Z \rangle$ of the ancillary qubit. Here, $U_k = T_k S_k^\dagger$ and $U_q = T_q S_q^\dagger$. In the figure, we assume that $k < q$ and $q = L + 1$.

-
- [1] R. P. Feynman, Simulating physics with computers, *International Journal of Theoretical Physics* **21**, 467 (1982).
- [2] S. Lloyd, Universal quantum simulators, *Science* **273**, 1073 (1996).
- [3] A. Y. Kitaev, Quantum measurements and the abelian stabilizer problem (1995), arXiv:quant-ph/9511026 [quant-ph].
- [4] Y. Dong, L. Lin, and Y. Tong, Ground-state preparation and energy estimation on early fault-tolerant quantum computers via quantum eigenvalue transformation of unitary matrices, *PRX Quantum* **3**, 040305 (2022).
- [5] H. F. Trotter, On the product of semi-groups of operators, *Proceedings of the American Mathematical Society* **10**, 545 (1959).
- [6] N. Hatano and M. Suzuki, Finding exponential product formulas of higher orders, in *Quantum Annealing and Other Optimization Methods*, edited by A. Das and B. K. Chakrabarti (Springer Berlin Heidelberg, Berlin, Heidelberg, 2005) pp. 37–68.
- [7] Y. Kim, A. Eddins, S. Anand, K. X. Wei, E. Van Den Berg, S. Rosenblatt, H. Nayfeh, Y. Wu, M. Zaletel, K. Temme, *et al.*, Evidence for the utility of quantum computing before fault tolerance, *Nature* **618**, 500 (2023).
- [8] A. Katabarwa, K. Gratsea, A. Caesura, and P. D. Johnson, Early fault-tolerant quantum computing, *PRX Quantum* **5**, 020101 (2024).
- [9] S. Khatri, R. LaRose, A. Poremba, L. Cincio, A. T. Sornborger, and P. J. Coles, Quantum-assisted quantum compiling, *Quantum* **3**, 140 (2019).
- [10] J. McClean, S. Boixo, V. Smelyanskiy, R. Babbush, and H. Neven, Barren plateaus in quantum neural network training landscapes, *Nature Communications* **9** (2018).
- [11] K. Mizuta, Y. O. Nakagawa, K. Mitarai, and K. Fujii, Local variational quantum compilation of large-scale hamiltonian dynamics, *PRX Quantum* **3**, 040302 (2022).
- [12] S. Kanasugi, Y. Hidaka, Y. O. Nakagawa, S. Tsutsui, N. Matsumoto, K. Maruyama, H. Oshima, and S. Sato, Subspace-based local compilation of variational quantum circuits for large-scale quantum many-body simulation (2024), arXiv:2407.14163 [quant-ph].
- [13] Y. Li and S. C. Benjamin, Efficient variational quantum simulator incorporating active error minimization, *Phys. Rev. X* **7**, 021050 (2017).
- [14] X. Yuan, S. Endo, Q. Zhao, Y. Li, and S. C. Benjamin, Theory of variational quantum simulation, *Quantum* **3**, 191 (2019).
- [15] K. Bharti and T. Haug, Quantum-assisted simulator, *Phys. Rev. A* **104**, 042418 (2021).
- [16] Y.-X. Yao, N. Gomes, F. Zhang, C.-Z. Wang, K.-M. Ho, T. Iadecola, and P. P. Orth, Adaptive variational quantum dynamics simulations, *PRX Quantum* **2**, 030307 (2021).
- [17] A. McLachlan, A variational solution of the time-dependent schrodinger equation, *Molecular Physics* **8**, 39 (1964).
- [18] K. Mitarai and K. Fujii, Methodology for replacing indirect measurements with direct measurements, *Phys. Rev. Res.* **1**, 013006 (2019).
- [19] M.-D. Choi, Completely positive linear maps on complex matrices, *Linear Algebra and its Applications* **10**, 285 (1975).
- [20] A. Jamiolkowski, Linear transformations which preserve trace and positive semidefiniteness of operators, *Reports on Mathematical Physics* **3**, 275 (1972).
- [21] X.-Z. Luo, J.-G. Liu, P. Zhang, and L. Wang, Yao.jl: Extensible, Efficient Framework for Quantum Algorithm Design, *Quantum* **4**, 341 (2020).
- [22] X. Wang, Z. Sun, and Z. D. Wang, Operator fidelity susceptibility: An indicator of quantum criticality, *Phys. Rev. A* **79**, 012105 (2009).
- [23] G. Gour, Comparison of quantum channels by superchannels, *IEEE Transactions on Information Theory* **65**, 5880 (2019).